https://doi.org/10.48047/AFJBS.6.15.2024.10542-10562

African Journal of Biological Sciences

Journal homepage: http://www.afjbs.com

Research Paper Open Access

Structure, NBO, NCI and spectrum analysis of a Phenylpropenoid molecule hosted at βeta-Cyclodextrin cavity

Houria Bouchemella[(1)],Fatiha Madi[(2)] ,Leila Nouar[(2)]

(1)Computational Chemistry and Nanostructures Laboratory, Department of Process Engineering, Faculty of Science and Technology, University of May 08, 1945, Guelma, Algeria.
(2) Computational Chemistry and Nanostructures Laboratory, Department of Material Sciences, Faculty of Mathematics, Computer Science and Material Sciences, University of May 08, 1945, Guelma, Algeria.

E-mail: bouchemella_h@hotmail.it

Volume 6, Issue 15, Sep 2024

Received: 15 July 2024

Accepted: 25 Aug 2024

Published: 25 Sep 2024

doi:10.48047/AFJBS.6.15.2024.10542-10562

Abstract

The density functional theory -DFT- at the theoretical level B3LYP/ 6-31G and ωB97-XD/6-31G in vacuum and in water was used for the study of the inclusion complex of Trans-Anethole (T-An) in to β-Cyclodexrin (β-CD) in two orientations A and B. The results indicate that the most favorable structure from an energetic point of view is when the propenyl group enters the cavity of the (β-CD) through its wide cavity, hence the methoxy group is positioned on the narrow side thereof with complete insertion of the benzene group. Donor-acceptor interactions between guest and host, studied using natural bonding orbital (NBO) analysis show the presence of weak and strong intermolecular hydrogen bonds in addition to van der Waals interactions. The spectral analysis of the ^{1}HNMR proton discussed with NBO results confirm the mutual interactions between T-An. and (β-CD). Also, the comparison of the theoretical and experimental UV spectra showed a good agreement thus justifying the appropriateness of the theoretical process undertaken in the modeling of this inclusion complex as affirmed by infrared spectroscopy and NCI analysis.

.***Keywords****: Trans-Anethole@β-CD,DFT,GIAO-^{1}HNMR, NBO, TD-DFT, NCI.*

1. Introduction

Anetholeis in the class of phenylpropanoid organic compounds, used for therapeutic and other purposeshas a pleasant taste even in high concentrations, and it is thirteen times sweeter than sugar. Trans-Anethole contains in its structure an aromatic nucleus para-substituted by a propenyl chain (C_3H_5) and a methoxy group ($O\text{-}CH_3$);it exists in the form of two isomers Cis (S) and Trans (E) according to the configuration of the double bond of the propenyl group,due to the high toxicity of Cis-Anethol, only Trans-Anethole(T-An)is used[1].

Trans-Anethole has antiviral activities,insect repellent, anti-inflammatory, antispasmodic activity;itis also used as a masking agent in toilet soap, toothpaste, as a flavoring and fragrance additive in food industry products such as candies [2-6].

Basically, Trans-Anethole like all phenylpropanoids have low water solubility and are sensitive to heat, light and free radicals, their encapsulation in Cyclodextrins improves their solubility and their stability and maintains their bioactivity[7].

B-Cyclodextrin isa cyclic oligosaccharide composed of α-D-glucopyranose units. It is composed of 7 α-1,4-glycosidic bonds and has the property of forming inclusion complexes with various guest molecules with suitable polarity and dimension improving their solubility, stability and bioavailability, because of its specialmolecular structure of the hydrophobic internal cavity which is shaped like a truncated cone of about 8 Å deep and 6.0–6.4 Å in diameter and the hydrophilic external surface [8-10].

Recently, several experimental studies of the complexation of Trans-anethole in β-Cyclodextrinhave been carried out in physical, in water and in ethanol mixtures,however, astructural study of the complexation of Trans-Anethole with β-Cyclodextrinconducted by Kfoury[11] et al. and Zhang [12] et al. did not elucidate the driving and physical forces leading to its formation.

The main objective of this work is to provide a general overview of the modifications of the properties: structural, spectral and the intermolecular interactions established between T-An. and β-CD during the formation of the inclusion complex.

2. Computational details

In this work, all quantum calculations are done with the program Gaussian 09 D01 [13] and Gauss View[14] using the density functional theory DFT method [15].The structure of the T-An molecule was constructed using the graphical interface of the Hyperchem 7.5 software [16], the geometry of the β-CD was extracted from the

Chem-Office 3D ultra software [17].After which, the two molecules were optimized,Fig.1shows the chemical structures of T-An. Andβ-CD optimizedat B3LYP/6-31G level of theory. The T-An@β-CD inclusion complex with stoichiometry 1:1 is constructed by introducing the guest molecule inside the cavity of the β-CD so that the interglycosidicoxygenof the β-CD are placed in the XY plane and the guest molecule is aligned along the z axis.

Two orientations are constructed: Orientation A; the methoxy O-CH_3 group of T-An. points to the wide portal of β-CD and in orientation B; the propenyl group $C_3H_5$of guest molecule points to the wide portal of β-CD as illustrated in Fig.2.

These two orientations are then optimized without any restrictions at the functional of exchange-correlation B3LYP [18-20] and ωB97-xD [21, 22] levels of theory with 6-31G basis set in gas and aqueous phases. The solvent effects have been taken into account in water (ε = 78.5) by a conductor polarizable continuum model (CPCM) [23].Harmonic vibrational frequencies were computed for the minimum energy structures to verify them to be at the minimum on the potential surface. The gauge-independent atomic orbital (GIAO) method as implemented in Gaussian was used to compute ^{1}H NMR chemical shifts of free and complexed guest and host molecules. Electronic transitions by time-dependent density functional theory (TD-DFT) and the frequency shift in the calculated vibrational spectra were explained.

Finally, NCI-RDG analysis were envisaged using the Multiwfnprogram [24] and visualized by the VMD program [25]to visualize weak interactions between the host and guest molecules.

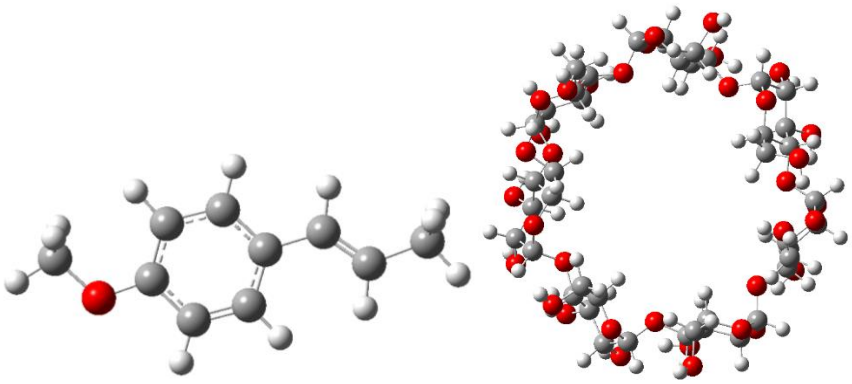

Fig. 1. Chemical structures of T-An. and β-CD optimized at B3LYP/6-31G level of theory.

.

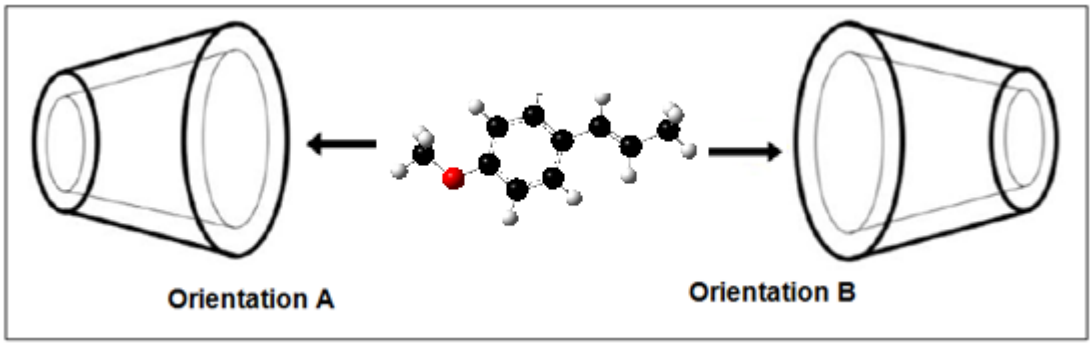

Fig. 2. Structures proposed for the inclusion of T-An in β-CD according to the two orientations A and B.

3. Results and discussions

3.1 Analysis of the different energy components and stability of the complex

The first part of our study concerns the calculation of stabilization, interaction and deformation energies of a complex as well as the energy gap ΔE(E_{HOMO}-E_{LUMO}) as well as the dipole moment of the complex T-An@β-CD according to the two orientations.

The stabilization energyfor the complex are given by the formula below:

$$\Delta E_{S.E.} = E^{opt}_{T-AN@\beta-CD} - \left(E^{opt}_{T-AN,libre} + E^{opt}_{\beta-CD,libre}\right) \quad (1)$$

The interaction energy estimates the distortion of the two molecules during complexationis calculated from the equation [26, 27]:

$$\Delta E_{interaction} = \left(E^{opt}_{T-AN} + E^{opt}_{\beta-CD}\right) - (E^{sp}_{T-AN} + E^{sp}_{\beta-CD}) \quad (2)$$

Where$E^{opt}_{T-An@\beta-CD}$is the energy of optimized inclusion complex,E^{opt}_{T-An},$E^{opt}_{\beta-CD}$ are energies of optimizedhost and guest moleculeand E^{sp}_{T-An}, $E^{sp}_{\beta-CD}$ aresingle point energy obtained for the distorted isolated molecule geometry upon complexation.The results obtained are summarized in Table 1.

From Table 1 it can be seen that the values of stabilization and interaction energies in gas phase and in water are all negative which indicate that the formed complexes are energetically favorable. In gas phase the complex T-An@β-CD (B) is most favorable with the stabilization energy (-31.25, -1.34 kcal/mol)and this with the two functional B3LYP and ωB97-xD, in water the complex T-An@β-CD(B) is the most favorable orientation at the theoretical level B3LYP although with the functional ωB97-xD the complex T-An@β-CD(A) is more favorable with a slight difference in stabilization energy compared to the T-An@β-CD(B) complex equal to -0.38 kcal/mol, this can be

explained by the fact that the functional ωB97-xD is a long-range corrected DFT

Methods	B3LYP /6-31G	ωB97-xD /6-31G	B3LYP /6-31G	ωB97-xD /6-31G	B3LYP /6-31G	ωB97-xD /6-31G
	T-An		A	OA	B	B
In gas phase						
$\Delta E_{S.E.}$(kcal/mol)	/	/	-6.79	-28.68	**-11.34**	**-31.25**
$\Delta E_{interaction}$(kcal/mol)	/	/	-5.79	-39.71	-8.95	-36.71
$\Delta E_{(HOMO-LUMO)}$ (eV)	-0.1787	-0.31855	-4.8498	-9.0049	-4.997	-8.9490
μ (Debye)	1.455	1.486	6.803	6.0823	6.619	7.5861
In water						

functional with dispersion corrections like Van der Waals interactions.

$\Delta E_{(HOMO-LUMO)}$ is a parameter that translates both the stability and the light resistance of molecular systems. According to the values of $\Delta E_{(HOMO-LUMO)}$reported in the Table 1 are of the order of 5 eV at the theoretical level B3LYP and 9 eV at the theoretical level ωB97-xD, all models in vacuum and in water are closely stable, compared to T-An before complexation. The dipole moment measures the polarity of a molecule, this one is at the maximum in orientation B in water equal to 8.3976 (9.3668) Debye which confirms the improvement of solubility of guestmolecule after inclusion in the host one.

Table 1: Energies of stabilization, interaction, energy gap and the dipole moment of T-An@β-CD complex according to the two orientations.

$\Delta E_{SE.}$(kcal/mol)	/	/	-4.45	**-28.64**	-6.451	**-28.26**
$E_{interaction}$ (kcal/mol)	/	/	-4.00	-35.28	-5.59	-31.95
$\Delta E_{(HOMO-LUMO)}$ (eV)	-0.1788	-0.23185	-4.8609	-9.0220	-4.9838	-8.3668
μ (Debye)	1.888	1.934	7.745	8.2607	8.3976	9.3668

3.2 Geometric structures of the complex

According to Fig.3, the structures of the lowest energies obtained by optimization of the geometries of the two orientations A and B in vacuum and in water show a total penetration of the guest molecule, its propenyl and methoxy groups are held in interaction by the oxygens and hydrogens of the two portals of β-CD, whereas the hydrogens of the benzene ring are in interaction with the glycosidic oxygen atoms of the β-CD.All these intermolecular interactions have lengths less than 3Å typical of weak physical bonds (hydrogen, van der Waals, etc.). It is also noted that these lengths have undergone elongations or shrinkingof the order of 0.01 to 0.02 Å in water due to themodification in the polarity of the complex in water in both orientations.

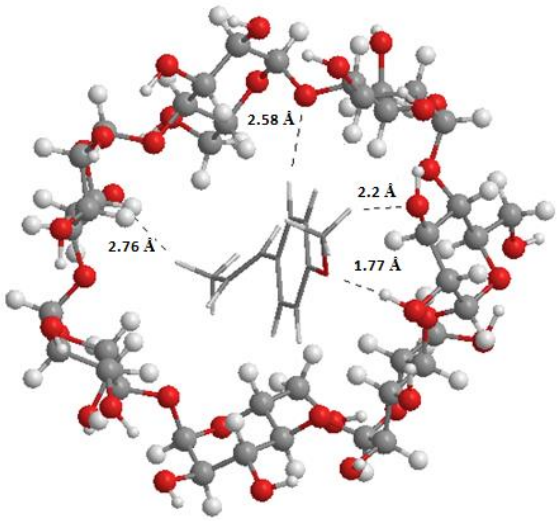

Orientation A in vacuum

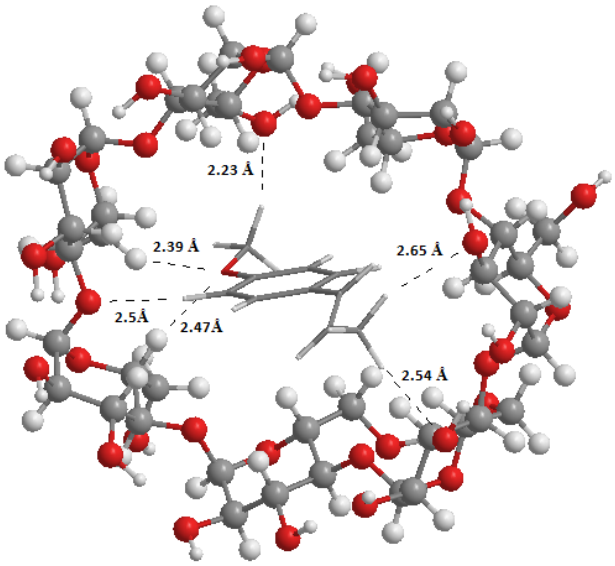

Orientation B in vacuum

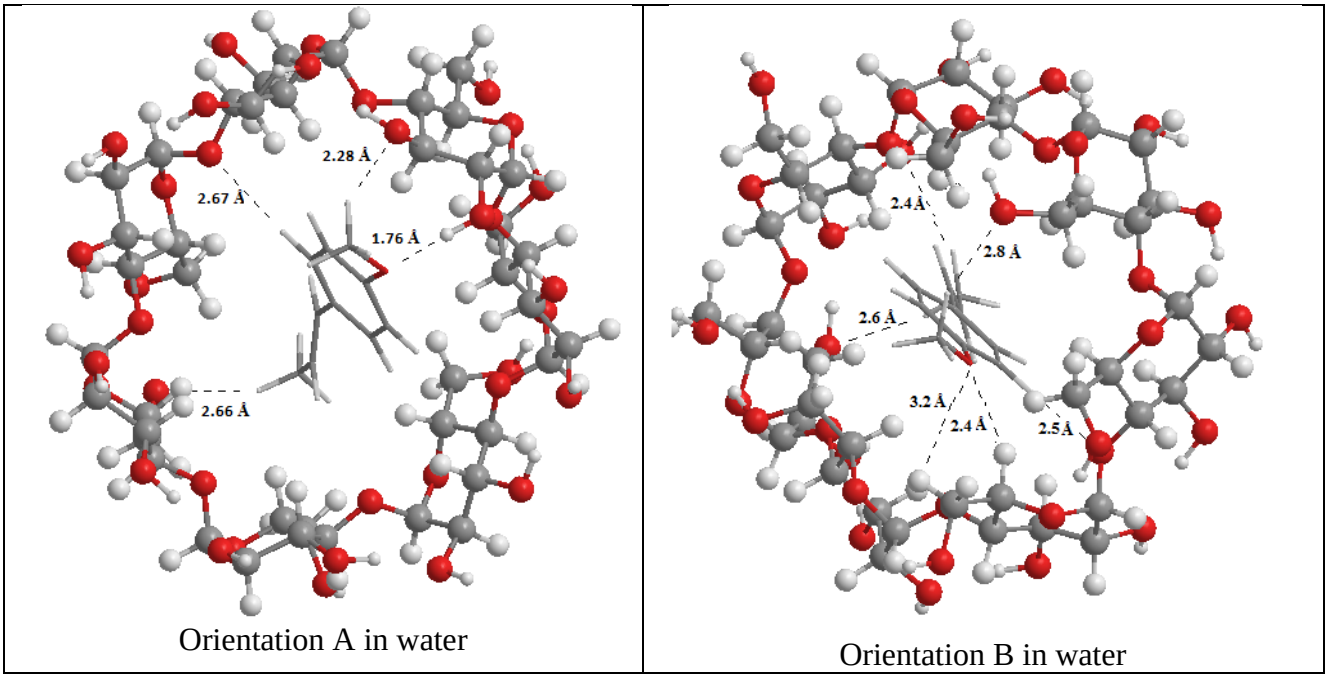

Orientation A in water

Orientation B in water

Fig.3. Geometric structures of the T-An@β-CD complex in vacuum and in water optimized by the ω97-xD/6-31G method.

3.3 NBO analysis

The non-covalent interaction is an interesting and stimulating research subject, to access it one generally resorts to NBO analysis which is a very powerful tool to study the interactions of the mutual hydrogen bond type between the different supramolecularmolecules and also provides a practical basis for studying charge transfer or conjugate interactions in this type of systems [28-31].

By definition, the stabilization energies resulting from the second-order micro-disturbance theory are reported according to the equation:

$$E^{(2)} = \mathrm{q_i}\frac{\mathrm{F(i,j)}}{\varepsilon\mathrm{j}-\varepsilon\mathrm{i}} \qquad (3<<<)$$

q_i : The occupation of the donor orbital.

F (i, j) : the Fock operator.

ε_i, ε_j : the energies of the NBO orbitals.

The larger the $E^{(2)}$ value, the shorter the interatomic distance. The delocalization of the electron density between the occupied NBO orbitals of the Lewis type (bonding or lone doublet) and the unoccupied non-Lewis orbitals NBO of the non-Lewis type (non-bonding or Rydberg) corresponds to a stabilizing donor-acceptor interaction.

Generally, an $E^{(2)}$ value greater than 2 kcal/mol is attributed to a strong hydrogen bond interaction and a value of 2 to 0.5 kcal/mol to a weak H bond interaction.

Table 2summarizes the NBO parameters for the most important interactions detected in the studied inclusion complex both in vacuum and in water for orientations A and B. The interaction energies and their corresponding distances show that the shorter the intermolecular distance, the greater the value of $E^{(2).}$

In both orientations A and B in vacuum and in water, the largest delocalization of electron densities are those arising from the lone electron pairs (LP) of the oxygen atom as donor electrons and OH as electron acceptors.

In orientation A, we note the presence of a strong intermolecular H bond corresponding to the electron donor-acceptor orbital LP O154→ BD*O59–H135, (between the free oxygen pair O154 of the methoxy group of T-An and the proton H135 located on the wide portal of the host molecule.) which stabilized the system up to 17.33 kcal/mol in vacuum and 19.99 kcal/mol in water.

In orientation B, the strongest intermolecular hydrogen bond type interaction corresponds to LP O47 → BD* C 155-H 164, (between the lone pair O47 located on the narrow portal of β-CD and the proton H164 of the groupmethoxy of T-An) which stabilizes the molecular structure at an energy equal to 5.22 kcal/mol in vacuum and 3.00 kcal/mol in water.

We conclude on reviewing Table 2 that the T-An@β-CD complex is stabilized due to a set of weak and strong hydrogen interactions.

Donor	Acceptor	$E^{(2)}$ (kcal/mol)	d (Å)	Donor	Acceptor	$E^{(2)}$ (kcal/mol)	d (Å)
A orientation in vacuum				B orientation in vacuum			
BD (2) C 148 - C 150	BD*(1) C 21 - H 100	1,63	2,57	LP (2) O 55	BD*(1) C 158 - H 170	1.38	2,65
LP (1) O 47	BD*(1) C 158 - H 169	0,83	2,76	**LP (1) O 47**	**BD*(1) C 155 - H 164**	**5,22**	**2,23**
LP (1) O 56	BD*(1) C 151 - H 161	1,41	2,58	LP (2) O 60	BD*(1) C 158 - H 169	1.82	2,54
LP (2) O 60	BD*(1) C 155 - H 164	**4,29**	2,28	LP (1) O 76	BD*(1) C 149 - H 159	1.84	2,49
LP(1) O154	BD*(1) O 59 - H 135	**6,34**	1,77	LP (1) O 154	BD*(1) C 35 - H 116	1.51	2,47
LP(2) O154	**BD*(1) O 59 - H**	**17,33**	1,7	LP (1) O	BD*(1) C 42 - H	1.83	2,39

	135		7	154	124		
A orientation in water				B orientation in water			
BD (2) C 148 - C 150	BD*(1) C 21 - H 100	**2,31**	2,65	LP (1) O 76	BD*(1) C 149 - H 159	1,69	2,52
LP (1) O 47	BD*(1) C 158 - H 169	1,27	2,66	LP (2) O 60	BD*(1) C 158 - H 169	1,74	2,56
LP (2) O 60	BD*(1) C 155 - H 164	**4,32**	2,22	**LP (1) O 47**	**BD*(1) C 155 - H 164**	**3,00**	**2,42**
LP (1) O 154	BD*(1) O 59 - H 135	**5.56**	1,76	LP (1) O 154	BD*(1) C 35 - H 116	1,92	2,41
LP (2) O 154	**BD*(1) O 59 - H 135**	**19,99**	1,76	LP (1) O 154	BD*(1) C 42 - H 124	**2,16**	2,34

Table 2: Natural bond orbital and the corresponding $E^{(2)}$ energies in T-An@β-CD inclusion complex at ωB97-xD/6-31G level of theory.

3.4 Spectral analysis by GIAO/^{1}HNMR

NMR is the most important analyzing instrument to verify the formation and the structure of inclusion complexes. In order to show the sensitivity of the hydrogens of the guest molecule to complexation, we calculated the chemical shifts of the different protons of T-An, β-CD free and in the complex using the Gauge Atomic Orbital approach GIAO [32]. The calculations were carried out at the theoretical level B3LYP/6-31G. The values of the ^{1}H chemical shifts (δ in ppm) were referenced to Tetra Methyl Silane (TMS) at the same theoretical level (δ=0.89) according to the equation:

$$\delta = \delta_H - \delta_{TMS} \qquad (4)$$

The effect of the H_2O solvent was modeled using the CPCM model.Fig.4.shows the T-An numbering system adopted in our work and that provided by Kfoury et al.[11]. The results obtained are summarized in Table 3 and Table 4 as well as Fig. 5.

Table 3 shows the theoretical and experimental shifts of T-An. andβ-CDafter complexation. It is noted that all the protons of the β-CD presented shifts towards the top fields in particular the protons H-3(121) and H-5(123) located inside its cavity with respective displacements of (-0.529/-0.73 ppm), (-0.247/-0.892 ppm) for orientation A/orientation Bconsequent to the formed van der walls and H-bonds interactions.

The proton H-6(124) located on the narrow portal of β-CD with a shift of (-0.127 /-0.173 ppm) in the orientation A/orientation B, these shifts are powerful evidence to confirm the formation of inclusion complexes [33, 34].

Table 4 summarizes the theoretical and experimental shifts obtained for T-An. and in the T-An@β-CD complex according to orientations A and B.

It is also noted that the proton signals in T-An also experienced changes in the included state, all protons exhibited either downfield or up field shifts, the largest shift in the A orientation is attributed to the protons Hf (0.4455 ppm) of the methoxy group and He (-0.4445 ppm) of the propenyl group, while for the B orientation the largest shift is attributed to the protons Ha (0.5598 ppm) of the benzene group and Hc (0.4516 ppm) of the propenyl group, which attests to the formation of physical bonds with the host molecule.Also, the theoretical and experimental displacements of the protons in the complex showed a good linear correlation as shown in Fig. 5.

To better illustrate the interactions responsible for the modification of the protons chemical shifts of T-An. we have shown all the donor-acceptor interactions obtained by the NBO calculations. (Table S1)

From Table S1 we can see that protons of T-An. interact with β-CD atoms as donor or acceptor of charges. For Hf(H163, H164 and H 165)and He(H168, H 169and H170) of T-An. on A orientation:

-H163 acts as donor with (RY*(1) H 135, 0.10kcal/mol),H164 interacts with (BD (1) O 60 - H 136, 0.15kcal/mol), (BD (1) O 60 - H 136, 0.18kcal/mol), (LP (1) O 60 , 0.83kcal/mol), (LP (2) O 60 , 4.29kcal/mol), (RY*(2) O 60 ,0.15kcal/mol),(RY*(1) H 135 , 0.09kcal/mol),(BD*(1) C 21 - O 60 ,0.09kcal/mol) and (RY*(2) O 60 ,0.15kcal/mol). Also, H 165 is in physic interaction with (RY*(1) H 135 , 0.09 kcal/mol).

-H168 is bounded to (BD (1) C 42 - H 124 ,0.14kcal/mol),(RY*(1) H 52, 0.11kcal/mol), (RY*(1) H 123, 0.14kcal/mol), (RY*(1) H 124 ,0.06kcal/mol), (BD*(1) C 12 - H 52, 0.08kcal/mol) and (BD*(1) C 42 - H 124 ,0.18kcal/mol) orbitals. Furthermore, H 169 is surrounded by (RY*(1) H 52 ,0.31kcal/mol),(RY*(1) H 123 , 0.29 kcal/mol), (BD*(1) C 5 - H 83 ,0.09 kcal/mol), (BD*(1) C 12 - H 52 ,0.22 kcal/mol), (BD*(1) C 41 - H 123, 0.39 kcal/mol), (BD (1) C 6 - H 85,0..06 kcal/mol), (BD (1) C 41 - H 123, 0.07 kcal/mol), (LP (1) O 47 ,0.83 kcal/mol). H170 is also in week interaction with (BD (1) C 41 - H 123 ,0.08 kcal/mol), (RY*(1) H 52, 0.20 kcal/mol), (RY*(1) H 123 ,0.09 kcal/mol), (BD*(1) C 12 - H 52 ,0.10 kcal/mol) and (BD*(1) C 41 - H 123 ,0.12 kcal/mol).

Thus we conclude that week interactions of T-An with atoms of β-CD are the origin of downfield or upfield protons shifts.

Table 3:[1]HNMR chemical shifts (ppm) of β–CD before and after complexation and experimental shifts

Protons B3LYP /6-31G	Calculated shift in (ppm)					Experimental shift in (ppm) [9]		
	$\delta_{\beta\text{-CD}}$	$\delta_{\beta\text{-CD}}$ Orientation A	Δδ	$\delta_{\beta\text{-CD}}$ Orientation B	Δδ	$\delta_{\beta\text{-CD}}$	$\delta_{\beta\text{-CD}}$ in Complex	Δδ
H(79) -1	4.445	4.380	-0.064	4.289	-0.156	5.074	5.045	-0.029
H(80) -2	3.025	2.901	-0.124	2.885	-0.14	3.651	3.625	-0.026
H(81) -3	3.216	2.686	-0.529	2.486	-0.73	3.968	3.919	-0.049
H(82) -4	2.314	2.178	-0.135	2.051	-0.263	3.587	3.564	-0.023
H(83) -5	3.621	3.373	-0.247	2.729	-0.892	3.880	3.791	-0.089
H(84) -6	3.065	2.938	-0.127	2.892	-0.173	3.880	3.847	-0.033

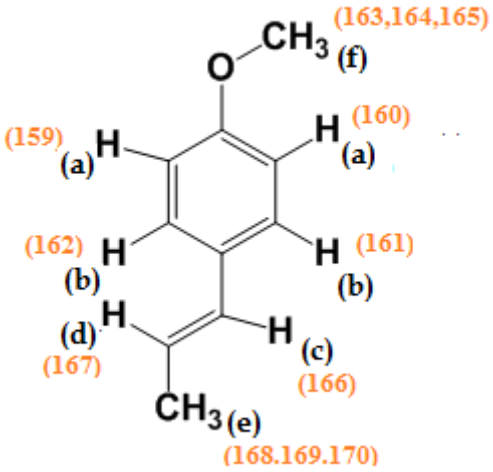

Fig. 4. T-Annumerotation in complex T-An@β-CD
Our work (in numbers) and as [9] (in alphabetical order).

Table 4:[1] HNMR chemical shifts (ppm) du T-An before and after complexation, calculated GIAO method at B3LYP/6-31G

Protons B3LYP	Calculated			Experimental [9]	
	$\delta_{\text{T-An}}$	$\delta_{\text{T-An in}}$ Orientation A	$\delta_{\text{T-An in}}$ Orientation B	$\delta_{\text{T-An}}$	$\delta_{\text{T-An}}$ in Complex
Aromatic: H162(Hb)	6.786	7.039	6.761	6.767	7.296
Aromatic:H161(Hb)	6.075	6.170	6.106	6.767	7.296
Aromatic:H159(Ha)	6.019	6.205	6.579	6.364	6.926
Aromatic: H160(Ha)	5.789	5.953	5.664	6.364	6.926
Propenyl:H167 (Hd)	5.652	5.679	5.706	5.601	6.168
Propenyl: H166(Hc)	5.592	5.461	6.044	5.896	6.376
Methoxy: H163(Hf)	3.297	3.274	3.094	3.154	3.812
Methoxy: H164(Hf)	2.982	3.333	3.294	3.154	3.812

Methoxy: H165(Hf)	2.982	2.999	2.886	3.154	3.812
Methyl: H168(He)	0.700	0.806	1.016	1.41	1.846
Methyl: H169(He)	1.162	1.509	1.477	1.41	1.846
Methyl: H170(He)	1.162	0.717	1.120	1.41	1.846

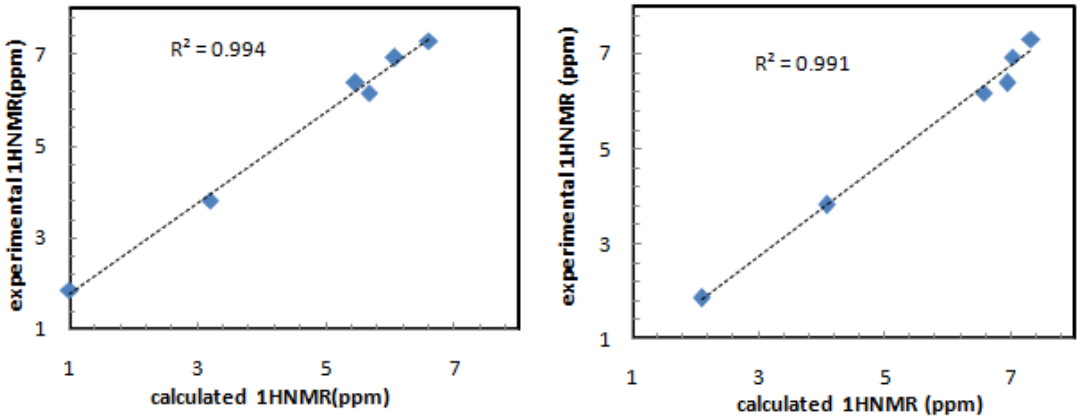

Fig.5. Correlation between calculated and experimental shifts at left in orientation A and in orientation B at right.

3.5 Analysis by infrared spectrometry

FT-IR is a helpful instrument to provide evidence for the formation of inclusion complexes. Widening, shifts and intensity change of the peaks indicate complex formation [35, 36]. Fig. 6shows the superposition of the infrared spectra of T-An, β-CD and in the complex T-An@β-CD in orientation A and B.

From Fig.6, there is a shift from the peak at 1010 cm^{-1} in free β-CDto 973 cm^{-1} and 964 cm^{-1} in complexes A and B respectively, also in the region of 1500 cm^{-1} at 500 cm^{-1} there are notable modifications in the shape of the theoretical peaks in comparison with that of the free β-CD.

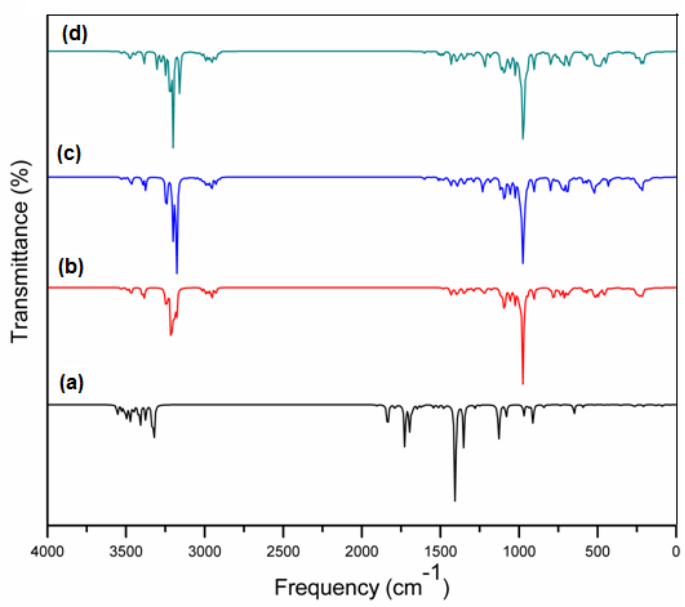

Fig. 6. Simulated infrared spectrum (a) T-An, (b)-β-CD, (c)-T-An@β-CD (A), (d) T-An@β-CD (B).

3.6 TD-DFT and theoretical UV-visible spectra

UV-visible spectroscopy is an important tool for studying inclusion complexes. Time-dependent density functional theory (TD-DFT) used for the calculation of the excitation energies and oscillator forces of molecules combines the advantages of the density functional theory and the time-dependent formalism allowing thus the precise determination of the properties of the excited state [37-39].

For this purpose we performed a calculation of the electronic transitions and their corresponding energies with the time-dependent density functional theory (TD-DFT) at B3LYP/6-31Gtheoretical level from the optimized structures. The effect of the solvent was taken into account with the model (CPCM) at the same theoretical level in water and in ethanol.

Fig. 7andFig. 8show a superposition of the absorption spectra of β-CD, T-An. and their inclusion complexes in the two orientations A and B.According to W. Zhang et al.[12], the anhydrous ethanol solution of β-CDhas no UV absorption, as well as the aqueous solution of β-Cylodextrin whereas the T-An in the Anhydrous ethanol exists in a $\lambda_{max}$of 260nm. From Fig.7andFig.8, it is observed that T-An exhibits a peak at 258.62 nm in water and a peak at 259.373 in ethanol. Free β-CD shows no absorption. It is clear that the spectra of T-An. present two absorption bands similar to those of the complex in both orientations. An isosbestic point in the T-An. spectrum due to the formation of the solute-solvent complex. While the isosbestic point appearing on the

spectrum of T-An in the presence of β-CD confirming the formation of the inclusion complex. The two bands of the complex are less intense than those of the free T-An.

The theoretical spectra of the T-An@β-CD inclusion complex according to the two orientations are as follows:

According to Table 5,orientation A showed 3 absorption peaks whose maximum is at 259.3 nm in water and at 259.41 nm in ethanol due to the excitation of HOMO→LUMO and HOMO→LUMO+1 respectively.Orientation B also showed 3 absorption peaks whose maximum is at 258.36 in ethanol due to HOMO→LUMO excitation and in water the excitation maximum is at 259.30 nm due to excitation HOMO →LUMO and HOMO→LUMO+1. The other excitation wavelengths with their peaks in water and ethanol are shown in the Table5.From Fig S.1 Intra and inter molecular charges transfer is observed between T-An and β-CD.

Thus, the UV analysis has perfectly justified the appropriateness of the theoretical process undertaken in the modeling of this inclusion complex where a good agreement has been verified.

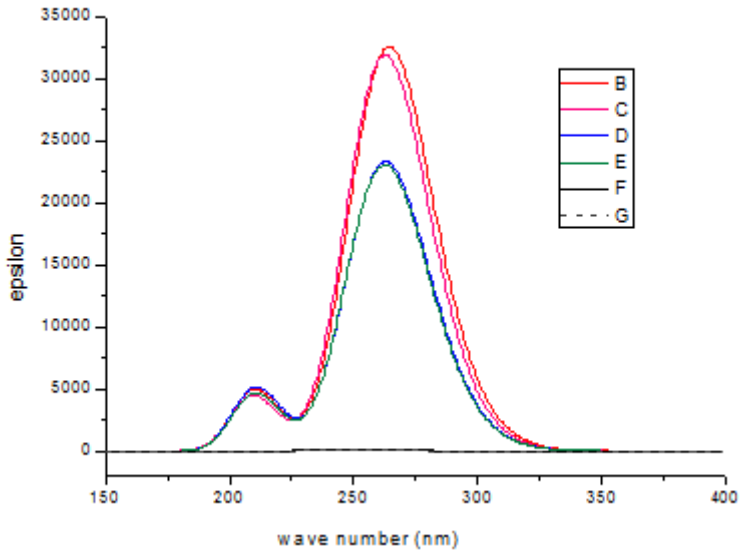

Fig.7. Simulated absorption spectra of: **(B)** T-An in Alcohol, **(C)**T-An in water, Orientation A: **(D)** T-An@β-CD in Alcohol, **(E)** T-An@β-CD in water, **(F)** β-CD in Alcohol and **(G)** β-CD in water.

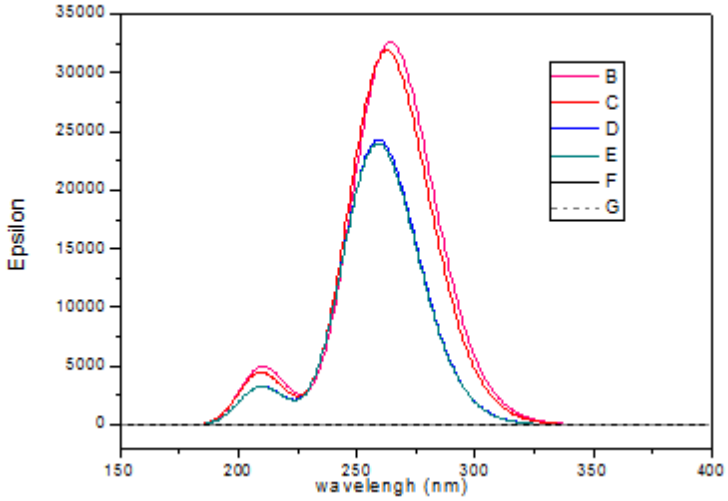

Fig. 8. simulated absorption spectra of: **(B)** T-An in Alcohol, **(C)** T-An in water, Orientation B : **(D)** T-An@β-CD in Alcohol, **(E)** T-An@β-CD in water, **(F)** β-CD in Alcohol and **(G)** β-CD in water

Excited state	Transition	Contribution %	E (eV)	f	λ (nm)
T-An@β-CD -A Orientation in Ethanol					
ES(1)	H-1→L H→L	6.14 52.87	4.5703	0.2021	271.28
ES(2)	**H→L** **H→L+1**	**45.41** **44.23**	**4.7795**	**0.4092**	**259.41**
ES(3)	H-3→L H-1→L H→L+1	2.13 75.48 11.84	5.8819	0.1267	210.79
T-An@β-CD -A Orientation in water					
ES(1)	H-1→L H→L	6.22 50.70	4.5693	0.1870	271.34
ES(2)	**H→L** **H→L+1**	**47.56** **42.59**	**4.7816**	**0.4175**	**259.30**
ES(3)	H-1→L H→L+1	72.63 10.69	5.8865	0.1144	210.62
T-An@β-CD -B Orientation in Ethanol					
ES(1)	H→LH→L +1	11.60 75.24	4.6308	0,0720	267.74
ES(2)	**H→L**	**86.38**	**4.7989**	**0.5388**	**258.36**
ES(3)	H-6→L+1 H-1→L H→L+1	3.56 73.18 10.30	5.9092	0.0812	209.82
T-An@β-CD -B Orientation in water					
ES(1)	H-1→L H→L	6.22 50.77	4.5693	0.1870	271.34
ES(2)	**H→L** **H→L+1**	**47.56** **42.59**	**4.7816**	**0.4175**	**259.30**
ES(3)	H-1→L H→L+1	72.63 10.69	5.8865	0.1144	210.62

Table 5: Transition between molecular orbitals corresponding wavelengths, energy and oscillatory strength (*f*)ofT-An@β-CD inclusion complex.

3.7 Non-Covalent Interaction (NCI) Analysis

Graphical illustration of weak intermolecular interactions such as hydrogen bonds, van der Waals interactions and repulsive steric interactions can be characterized by the method of non-covalent interaction NCI analysis [40-42]which provides a real-space graphical visualization of weak interactions.

To explore the existence of weak interactions, NCI plots are generated with the plots of the RDG versus (signλ2)ρ, where (signλ2)ρ is the electron density multiplied by the sign of the second Hessian eigenvalue (λ2) [43, 44].

Van der Waals interactions are colored green, hydrogen bonds are colored blue, and areas with repulsive steric interactions are colored red.

The NCI isosurface illustrated in Fig. 9display the inclusion complexes in water for A and B orientations at ωB97-xD level theory. A green mostly attractive area between T-An andβ-CD is observed, it indicates the presence of van der Waals interactions. Also, a greenish blue color is observed which testifies to the presence of weak attractive bonds of the hydrogen type. In orientation A, a region of dark blue color is retained between the oxygenO154of T-An. and the hydrogen H135 of the wide portal of β-CD attributed to a strong hydrogen bond. In addition,intramolecular H-bondobserved between primary and secondary hydroxyls rims of β-CD.

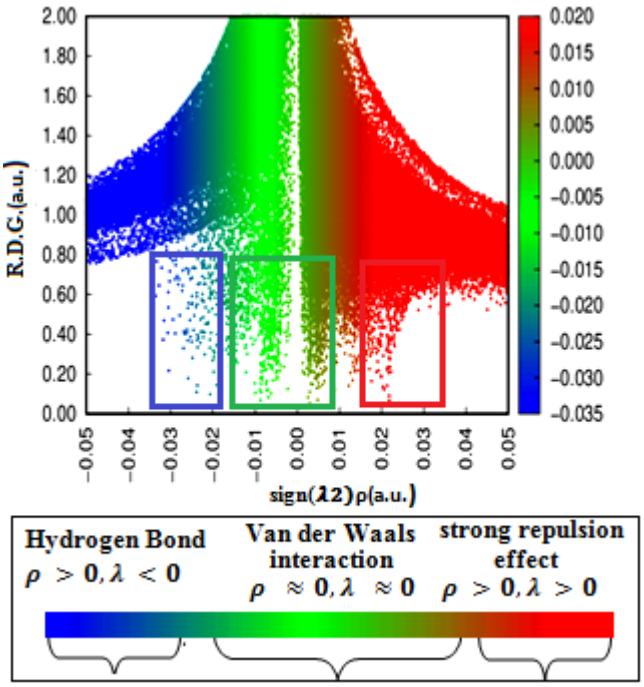
R.D.G.(a.u.)
sign(λ2)ρ(a.u.)
Hydrogen Bond
ρ > 0, λ < 0
Van der Waals interaction
ρ ≈ 0, λ ≈ 0
strong repulsion effect
ρ > 0, λ > 0

(a)

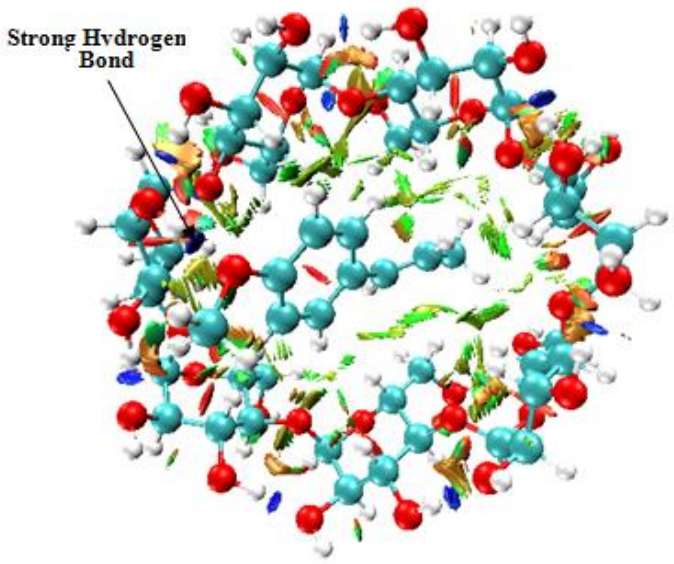
Strong Hydrogen Bond

(b)

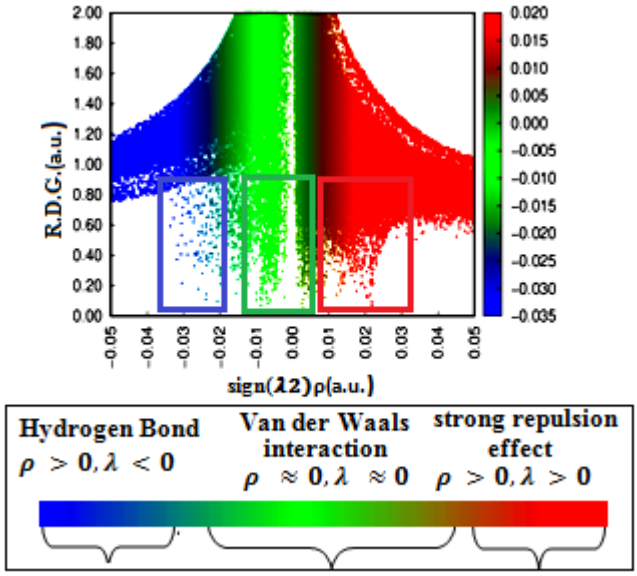

(c)

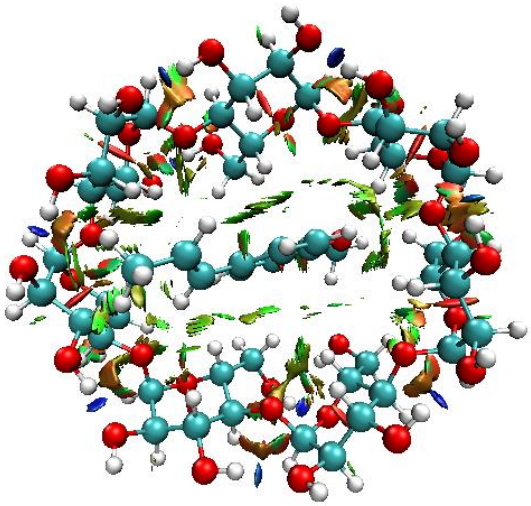

(d)

Fig. 9. Plot of the reduced density gradient versus the electron density mulitiplied by the sign of the second Hessian eigenvalue (signλ2)ρ and Visual weak interactions at ωB97-xD/6-31G level of theory (a), (b) in orientation A and (c) , (d) in orientation B.

4. Conclusion

B3LYP/ 6-31G and ωB97-XD/6-31G in vacuum and in water was used for the study of the inclusion complex of Trans-anethole (T-An) into β-Cyclodexrin (β-CD) in two orientations A and B. The obtained results showed that:

- Energetically, the formed inclusion complex is stable in A and B orientation in both vacuum and water with total of guest insertion in β-CD cavity.

-The established intermolecular interaction between T-An and β-CD obtained by NCI and NBO analysis are responsible of spectral properties modification (1HNMR, UV-visible and IR)

References

[1] G. Jashari, M.Frühbauerová,T.Mikysek, I.Švancara, R.Metelka,M.Sýs, New electroanalytical method for the determination of trans-anethole in spices and sweets, Food Chemistry 408(2023), https://doi.org/10.1016/j.foodchem.2022.135167

[2] A. Astani, J. Reichling, P. Schnitzler, Screening for Antiviral Activities of isolated compounds from Essential Oils, Evidence-Based Complementary and Alternative Medicine 2011 (2011), 253643,https://doi.org:10.1093/ecam/nep187

[3] M. Alkan, S. Ertürk, Insecticidal Efficacy and Repellency of Trans-AnetholeAgainst Four Stored-Product Insect Pests, Journal of Agricultural Sciences 26 (2019) 64-70,https://doi.org/10.15832/ankutbd.445671

[4] K. Y. Kim , H. S. Lee, G. H. Seol, Anti-inflammatory effects of trans-anethole in a mouse model of chronic obstructive pulmonary disease, Biomedicine & Pharmacotherapy91 (2017) 925-930,https://doi.org/10.1016/j.biopha.2017.05.032

[5] C. C.Lima,C. M. de Hollanda-Angelin-Alves., A. Pereira-Gonçalves, E. Kennedy-Feitosa, E. Evangelista-Costa , M. A. M. CarneiroBezerra, A. Coelho-de-Souza, J. H.

Leal-Cardoso, Antispasmodic effects of the essential oil of Croton zehnteneri, anethole, and estragole, on tracheal smooth muscle,Heliyon16 (2020), https://doi.org/10.1016/j.heliyon.2020.e05445
[6] V. Marinov, S. Valcheva-Kuzmanova, Review on the pharmacological activities of anethole,ScriptaScientificaPharmaceutica 2(2014) 14-19, https://doi.org/10.14748/ssp.v2i2.1141
[7] M. Kfoury, L.-H. Sahraoui, A. Bourdon, N. Laruelle, F. Fontaine, J. Auezova, L. greige-gerges, S. Fourmentin,Solubility, photostability and antifungal activity of phenylpropanoids encapsulated in cyclodextrins, Food Chemistry 196 (2015),https://doi.org/10.1016/j.foodchem.2015.09.078
[8]Li J, Xu F, Dai Y, Zhang J, Shi Y, Lai D, Sriboonvorakul N, Hu J. A Review of Cyclodextrin Encapsulation and Intelligent Response for the Release of Curcumin, *Polymers*14(24) (2022) 5421, https:/doi.org/10.3390/polym14245421
[9]Almeida B, Domingues C, Mascarenhas-Melo F, Silva I, Jarak I, Veiga F, Figueiras A. The Role of Cyclodextrins in COVID-19 Therapy—A Literature Review, *International Journal of Molecular Sciences* 24(3) (2023) 2974,https://doi.org/10.3390/ijms24032974
[10] B. G. Poulson, Q. A. Alsulami, A. Sharfalddin, E. F. ElAgammy, F. Mouffouk, A. H.Emwa, M. Jaremko,Cyclodextrins: Structural, chemical and physical properties and applications, Polysaccharides *3*(1) 2021, 1-31, https://doi.org/10.3390/polysaccharides3010001
[11] M. Kfoury, L.Auezova, H. Greige-Gerges, S. Ruellan, S. Fourmentin, Cyclodextrin, an efficient tool for trans-anethole encapsulation: Chromatographic, spectroscopic, thermal and structural studies,Food Chemistry164 (2014) 454–461, https://doi:10.1016/j.foodchem.2014.05.052
[12] W. Zhang, X. Li, T. Yu, L. Yuan, G. Rao, D. Li, C.Mu,Preparation, physicochemical characterization and release behavior of the inclusion complex of trans-anethole and β-cyclodextrin,Food Research International 74 (2015) 55-62, https://doi.org/10.1016/j.foodres.2015.04.029.
[13] M.J. Frisch, G.W. Trucks, H.B. Schlegel, G.E. Scuseria, M.A. Robb, J.R. Cheeseman, G.Scalmani, V. Barone, B. Mennucci, G.A. Petersson, H. Nakatsuji, M. Caricato, X. Li,H.P. Hratchian, A.F. Izmaylov, J. Bloino, G. Zheng, J.L. Sonnenberg, M. Hada, M.Ehara, K. Toyota, R. Fukuda, J. Hasegawa, M. Ishida, T. Nakajima, Y. Honda, O.Kitao, H. Nakai, T. Vreven, J.A. Montgomery Jr., J.E. Peralta, F. Ogliaro, M. Bearpark,J.J. Heyd, E. Brothers, K.N. Kudin, V.N. Staroverov, T. Keith, R. Kobayashi, J.Normand, K. Raghavachari, A. Rendell, J.C. Burant, S.S. Iyengar, J. Tomasi, M. Cossi,N. Rega, J.M. Millam, M. Klene, J.E. Knox, J.B. Cross, V. Bakken, C. Adamo, J.Jaramillo, R. Gomperts, R. Stratmann, O. Yazyev, A.J. Austin, R. Cammi, C. Pomelli,J.W. Ochterski, R.L. Martin, K. Morokuma, V.G. Zakrzewski, G.A. Voth, P. Salvador,J.J. Dannenberg, S. Dapprich, A.D. Daniels, O. Farkas, J.B. Foresman, J.V. Ortiz, J.Cioslowski, D.J. Fox, Gaussian 09, revision D.01, Gaussian, Inc, Wallingford, 2013.
[14] Dennington RI, Keith T, Millam J, GaussView Version 5.0.8.Semichem Inc.
[15] N. Argaman,G. Makov, Density functional theory: An introduction,*American Journal of Physics* 68 (1) (2000) 69–79, https://doi.org/10.1119/1.19375
[16] Hyperchem, Hypercube, Inc., USA, Hyperchem, Release 7.51 forWindows 2002, Hypercube.Inc.
[17] Chem-Office 3D ultra, Version 10, Cambridge Software 2006.

[18] A.D. Becke, Density-functional exchange-energy approximation with correct asymptotic behavior, Phy. Rev. A. 38 (1988) 3098–3100, https://doi.org/10.1103/PhysRevA.38.3098
[19] A. D. Becke, Density-Functional Thermochemistry. III. The Role of Exact Exchange, Journal of Chemical Physics, 98 (1993) 5648-5652, https://doi.org/10.1063/1.464913
[20] C. Lee, W. Yang, R.G. Parr,. Development of the Colle-Salvetti correlation-energy formula into a functional of the electron density,Phys Rev B,37(1988) 785-789, https://doi.org/10.1103/PhysRevB.37.785
[21] S. Grimme, Semiempirical GGA-type density functional constructed with a long-range dispersion correction, J. Comput. Chem. 27(2006) 1787-1799, https://doi.org/10.1002/jcc.20495
[22] J. Chai, M. Head-Gordon, Long-range corrected hybrid density functionals with damped atom-atom dispersion corrections. *Physical chemistry chemical physics 10 (2008)* 6615-6620,https://doi: 10.1039/b810189b
[23] M. Cossi, N. Rega, G. Scalmani, V.Barone, Energies, structures, and electronic properties of molecules in solution with the C-PCM solvation model, Journal of Computational Chemistry, 24(6) (2003), 669–681, https://doi.org/10.1002/jcc.10189
[24] T. Lu, F. Chen, Multiwfn: A Multifunctional Wavefunction Analyzer, Journal of Computational Chemistry, 33(2012) 580-592, https://doi.org/10.1002/jcc.22885
[25] W. Humphrey, A. Dalke, K. Schulten, VMD: Visual molecular dynamics, Journal of Molecular Graphics 14(1996) 33-38, https://doi.org/10.1016/0263-7855(96)00018-5.
[26] R. Kohli, R. P. Kaur**,** A Theoretical Study of Hydrogen-Bonded Complexes of Ethylene Glycol, Thioglycol and Dithioglycol with Water, Asian Journal of Chemistry 34 (2022), 169-182,https://doi.org/10.14233/ajchem.2022.23487
[27] C. Aleman, On the Ability of Modified Peptide Links to Form Hydrogen Bonds,*The Journal of Physical Chemistry A 105* (2001) 6717-6723, https://doi.org/10.1021/jp010198p

[28] A.E Reed, L.A. Curtiss, F. Weinhold, Intermolecular interactions from a natural bond orbital, donor-acceptor viewpoint, Chem. Rev. 88(1988), 899-926,https://doi.org/10.1021/cr00088a005
[29] F. Weinhold, C.R. Landis, Discovering Chemistry with Natural Bond Orbitals, John Wiley &Sons Inc (2012), DOI:10.1002/9781118229101
[30] S.J.Jenepha Mary, S. Pradhan, C. James , Molecular structure, NBO analysis of the hydrogen-bonded interactions, spectroscopic (FT-IR, FT-Raman), drug likeness and molecular docking of the novel anti COVID-2 molecule (2E)-N-methyl-2-[(4-oxo-4H-chromen-3-yl)methylidene]-hydrazinecarbothioamide(Dimer)-quantum chemical approach. SpectrochimActa A MolBiomolSpectrosc. 251(2021) 119388, https://doi.org/10.1016/j.saa.2020.119388
[31] S. Amrani, F. Madi, L. Nouar, Effect of solvent on absorption and emission spectra of 2,2′-Bipyridine and its inclusion complexintoβ-cyclodextrin: DFT and TD-DFT study, Computational and Theoretical Chemistry 1206 (2021) 113481, https://doi.org/10.1016/j.comptc.2021.113481
[32] G. Schreckenbach, T. Ziegler, Calculation of NMR Shielding Tensors Using Gauge-Including Atomic Orbitals and Modern Density Functional Theory, the journal of chemical chemistry 99(1995) 606-611, https://doi.org/10.1021/j00002a024

[33] S. LizyRoselet, J. PremaKumari, 1H NMR – A validation tool for supramolecular complexes of α-cyclodextrin with Antidiabetic drugs, Materials Today: Proceeding 37(2021) 88-93, https://doi.org/10.1016/j.matpr.2020.04.077
[34] Y. Chen, A. Mensah, Q. Wang, L. Dawei , Q. Yuyu, W. Qufu , Hierarchical porous nanofibers containing thymol/beta-cyclodextrin: Physico-chemical characterization and potential biomedical applications, Materials Science and Engineering C: 115(2020), 111155, https://doi:10.1016/j.msec.2020.111155
[35] L. Prakash Verma, P. ShridharGejji,Electronic structure and spectral characteristics of alkyl substituted imidazolium based dication-X2 (X = Br, BF4, PF6 and CF3SO3) complexes from theory, Journal of Molecular Liquids 293(2019) 111548, https://doi.org/10.1016/j.molliq.2019.111548
[36] D. Koyeli , R. N. Patra, L. R. Gardas, Study on inclusion complexation of β-CD and nitro-benzyl-imidazolium-based ionic liquids with various physicochemical techniques, Journal of Molecular Liquids 348 (2022) 118039, https://doi.org/10.1016/j.molliq.2021.118039
[37] N. S. Singh, S. M. Devi, Computational Exploration of 1-Amidino-O-(n-butyl) Urea (ABnUH) with Natural Atomic Orbitals, Natural Bond Orbital, Vibrational Analysis and Simulated UV-Visible Spectra, Asian Journal of Chemistry 33 3089-3098, https://doi.org/10.14233/ajchem.2021.23438
[38] D. Guillaumont, S. Nakamura, Calculation of the absorption wavelength of dyes using time-dependent density-functional theory (TD-DFT), Dyes and Pigments, 46(2000), 85–92, https://doi.org/:10.1016/S0143-7208(00)00030-9
[39] S. Panda, S. Nayak, P. K.DasD.L.Singh, Impact of Inclusion Complex Formation on Absorption and Emission Characteristics of Some 4-Arylidenamino-5-phenyl-4H-1,2,4-triazole-3-thiols, Asian Journal of Chemistry, 28 (2016) 981–986, https://doi:10.14233/ajchem.2016.19556
[40] U. Koch, P.L.A. Popelier, Characterization of C-H-O Hydrogen Bonds on the Basis of the Charge density, J. Phys. Chem. 99(1995) 9747–9754, https://doi.org/10.1021/j100024a016
[41] E.R. Johnson, S. Keinan, P. Mori-Sánchez, J. Contreras-García, A. J. Cohen, W. Yang, Revealing Noncovalent Interactions, Journal of the American Chemical Society 132 (2010), 6498-6506, https://doi.org/10.1021/ja100936w
[42] G. B. González, J. M. Espinoza, Thermodynamic and reactivity aspect of β-cyclodextrin inclusion complexes with coumarin derivatives, Journal of the Chilean Chemical Society67(2022) 5514-5520, https://doi.org/10.4067/S0717-97072022000205514
[43] M. Medimagh, N. Issaoui, S. Gatfaoui, A.S. Brandán, O. Al-Dossary, H. Marouani, J.W. Marek, Impact of non-covalent interactions on FT-IR spectrum and properties of 4-methylbenzylammonium nitrate. A DFT and molecular docking study, Heliyon 7(10) (2021), https://doi.org/10.1016/j.heliyon.2021.e08204
[44] N.S. Venkataramanan, A.Suvitha Y. Kawazoe, Density functional theory study on the dihydrogen bond cooperativity in the growth behavior of dimethyl sulfoxide clusters, Journal of Molecular Liquids 249 (2018) 454-462, https://doi.org/10.1016/j.molliq.2017.11.062